

Flow around three rectangular prisms between two walls

Ramnarayan Mondal^{*,1)}, Md. Mahbub Alam²⁾, Rajesh Bhatt³⁾, Qinmin Zheng⁴⁾ and Chunning Ji⁵⁾

^{1,2,3,4)} *Institute for Turbulence-Noise-Vibration Interaction and Control, Harbin Institute of Technology, Shenzhen, Shenzhen 518055, China*

⁵⁾ *State Key Laboratory of Hydraulic Engineering Simulation & Safety, Tianjin University, Tianjin, 300072, China*

²⁾ alamm28@yahoo.com; alam@hit.edu.cn

ABSTRACT

The flow around three side-by-side identical rectangular prisms (aspect ratio $b/h = 3$) placed between two parallel walls is studied numerically at a Reynolds number $Re = 100$, where b and h are the width and height of a prism, respectively. The effect of the cylinder gap spacing ratio $g^* = g/h$ ($= 0.8-3.2$) is investigated on Strouhal number (St), time-mean drag coefficient (\bar{C}_D), and fluctuating lift coefficient (C'_L). Structured quadrangular grid is used to solve unsteady Navier-Stokes equations, and pressure implicit with the splitting of operators (PISO) is employed to handle the coupling of pressure and velocity. It is observed that g^* substantially influences St , \bar{C}_D and C'_L which increase with decreasing g^* .

NOMENCLATURE

Re	Reynolds number ($\rho U_\infty h / \mu$)
U_∞	Free stream velocity
μ	Kinematic viscosity
ρ	Density of fluid
h, b	Height and width of prism
p	Pressure
St	Strouhal number
C'_L	Fluctuating lift coefficient
\bar{C}_D	Time-mean drag coefficient
g	Gap spacing between two prisms

1. INTRODUCTION

Cylindrical structures subjected to flow have been studied extensively because of their enormous applications in engineering such as chimney stacks, tube bundles in heat exchangers, spar platform, and undersea pipelines. On the other hand, it is equally important to understand the flow physics around a group of rectangular structures, e.g. flow past high rise buildings, suspension bridge, etc. Vortex shedding and wake formation behind different numbers of square cylinders in side-by-side arrangement were investigated in a number of numerical studies (Agarwal *et al.* 2006,

Kumar *et al.* 2008, Sewatkar *et al.* 2009, Alam *et al.* 2011, Alam and Zhou 2013, Zheng and Alam 2017). The dependence of the flow on gap spacing ratio g^* ($=g/h$) was focused in the studies. The studies were concerned with the unconfined flow where the side wall had negligible or almost no influence on the flow around the prisms. This unconfined flow is achieved when the blockage ratio is less than 6%. There are comparatively a small number of studies on the flow around rectangular prisms with side wall confinement. Davis *et al.* (1984) investigated the confined flow around a rectangular prism numerically and experimentally. The emphasis was given to understand the effect of blockage ratio, aspect ratio and Reynolds number on the wake of the rectangular prism. They observed that the Strouhal number and drag coefficient increase with increasing blockage ratio, i.e., when the side walls are brought close to the prism. Camarri and Giannetti (2007) carried out a numerical simulation to study the flow around a square prism centrally placed between two parallel walls with blockage ratios 1/6, 1/8 and 1/10. They examined the mechanism of vortex inversion and identification of the inversion position where the two opposite-sign vortices cross the line of symmetry. They pointed out that the incoming vorticity magnitude, confinement, and shape of the incoming flow play a significant role in the inversion. The inversion distance from the cylinder center shrinks monotonically when the blockage ratio and/or Reynolds number increases. For a given blockage ratio, the inversion distance was a linear function of Reynolds number for $Re \geq 110$.

Because of everything getting compact in the modern engineering, applications of the flow around multiple structures in wall proximity get broader, such as the flow around prisms/cylinders in a channel to enhance mixing and heat transfer, the flow around drive bays in CPUs, etc. Recently, fluid-structure instability has been identified in a CPU system having nine hard disks in a 3×3 arrangement. Some hard disks became out of order when the cooling-fan-driven air flow reached a certain level. It is believed that flow-induced oscillations of the disks are the main issue behind the disks not working. Naturally, investigations are direly needed on the flow around confined structures. To the best of the authors' knowledge, there is not a single study on the confined flow around multiple prisms in side-by-side arrangements. The objective of this study is to examine the influence of the side walls and gap spacing g^* on integral parameters St , C'_L and \bar{C}_D at $Re=100$ when fluid flows around three side-by-side rectangular (aspect ratio $b/h = 3$) prisms representing one column of the nine disks in the CPU. The gap distance ratio g^* between two consecutive prisms and between the outer prism and wall is varied systematically from 0.8 to 3.2.

2. PROBLEM DESCRIPTION AND CONVERGENCE STUDY

Three identical rectangular prisms (P_1 , P_2 and P_3) are placed in side-by-side arrangement between two parallel walls as shown in Fig. 1(a). The Cartesian coordinate system (x , y) is considered with the coordinate origin at the center of the middle prism, the x - and y -axis lying on the stream wise and cross-stream directions. The inlet and outlet faces are considered at distances $X_u = 16h$ and $X_d = 32h$ from the origin. The length of the domain of interest along lateral direction is Y_l . The governing

equations for unsteady, viscous, laminar and incompressible fluid flow are the conservation equations of mass and momentum, written in non-dimensional forms as

$$\nabla \cdot \mathbf{u}^* = 0 \quad (1)$$

$$\frac{\partial \mathbf{u}^*}{\partial t^*} + \mathbf{u}^* \cdot \nabla \mathbf{u}^* = -\nabla p^* + \frac{1}{Re} \nabla^2 \mathbf{u}^* \quad (2)$$

where $\mathbf{u}^* = (u^*, v^*)$ is non-dimensional velocity vector along the x and y directions respectively, such that $(u^*, v^*) = (u/U_\infty, v/U_\infty)$. The non-dimensional time (t^*) and pressure (p^*) are given by $t^* = tU_\infty/h$ and $p^* = p/\rho U_\infty^2$. The boundary conditions are summarized as follows. A uniform velocity profile is given at the inlet ($u^* = 1, v^* = 0$), while zero stress vectors ($2(\partial u^*/\partial x^*)=0, \mu(\partial v^*/\partial x^* + \partial u^*/\partial y^*)=0$) are specified at the outlet. Lastly, on the prism surfaces and the two side (upper and lower) walls, no-slip boundary conditions ($u^*=0, v^*=0$) are employed.

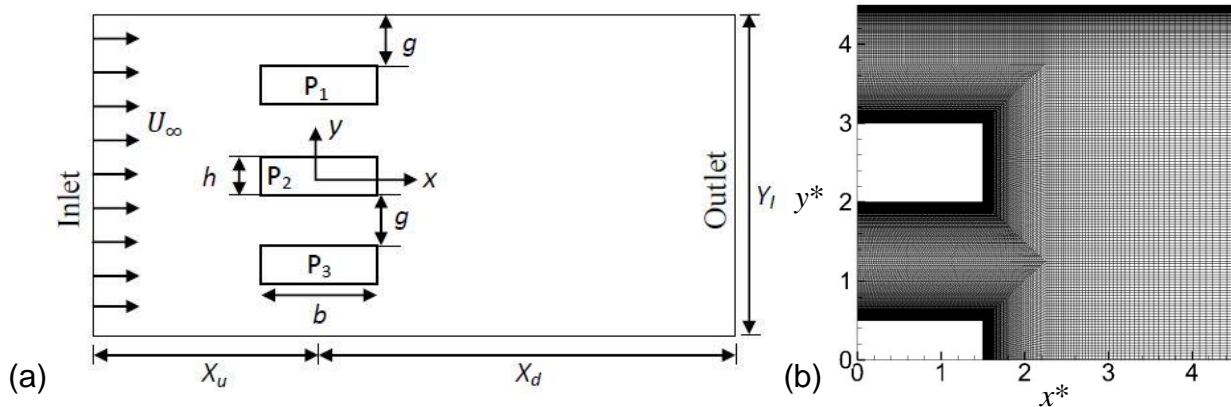


Fig. 1 (a) Sketch of the computational domain, and (b) grid structure around a quadrant of the computational domain.

Finite volume method based commercial software Ansys-Fluent is used to solve the governing Eqs. (1) and (2). The pressure implicit with splitting of operators (PISO) method is employed to handle the pressure velocity coupling. Convective terms are discretized using second order upwind scheme and fully implicit second order discretization is adopted for time marching.

Before proceeding to extensive simulation on three prisms, the mesh independence test is conducted for the flow around a square prism in an unconfined domain. Quadrangular grid is generated in the domain of interest using Ansys ICFD. The first node is set at a distance $0.005h$ from the prism surfaces as well as from the side walls for sufficient resolution of boundary layers. The grid spacing is increased with a geometric progression ratio of 1.03. The flow past a single square cylinder at $Re = 100$ is simulated first to confirm that the resolution in mesh is enough. Three different meshes ($M1 = 42564, M2 = 70880, M3 = 136548$) were considered. The results at $M2$

exhibited less than 5% deviation from those at the finest mesh M3 where the number of nodes at M3 is approximately twice that at M2. Therefore, mesh M2 was used for the extensive computation. In Table 1, St , C'_L and \bar{C}_D computed presently are compared with those in the literature. It is observed that there is a good agreement between the results. Therefore, the grid distribution for the single prism is adopted for the flow around three rectangular prisms. Fig. 1(b) shows the distribution of grids around a quadrant of computational domain for $g/h = 1.5$ with total number of nodes 226947. For other values of g^* , the number of nodes are increased or decreased accordingly.

Table 1 Comparison of present results with those in the literature for a square prism. $Re = 100$, $X_u/h = 16$, $X_d/h = 32$, $\Delta t^* = 0.0519$, blockage ratio = 5%.

	St	C'_L	\bar{C}_D
Present	0.1444	0.1845	1.4948
Sohankar <i>et al.</i> (1998)	0.1460	0.1560	1.4770
Sharma and Eswaran (2004)	0.1488	0.1922	1.4936
Sahu <i>et al.</i> (2009)	0.1486	0.1880	1.4878
Sen <i>et al.</i> (2011)	0.1452	0.1928	1.5287
Singh <i>et al.</i> (2009)	0.1470	0.1600	1.5100

3. RESULTS AND DISCUSSION

In this section, effects of g^* on Strouhal number, time-mean drag and fluctuating lift coefficients are discussed. From the power spectra (not shown here), it was observed that the three prisms have the identical St for the range of $g^* = 0.8 - 3.2$. Fig 2 shows the variation of St as a function of g^* . The St declines with increasing g^* . As the gap spacing ratio g^* decreases, the velocity through the gaps increase, leading to an increased St . From Fig. 2, it is observed that the shedding frequency decreases at a smaller rate as g^* increase. Similar phenomenon was observed by Zheng and Alam (2017) for three square prisms in unconfined flow.

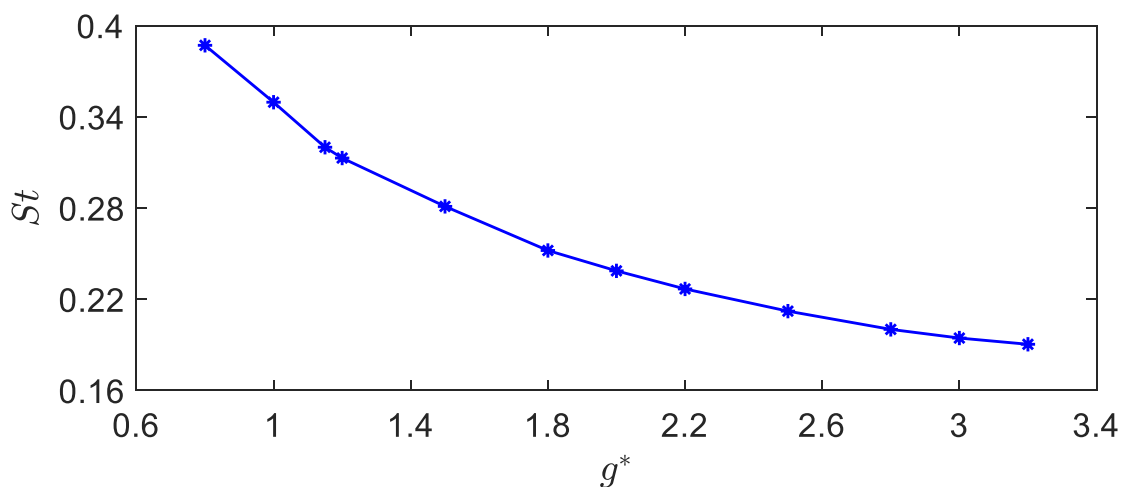


Fig. 2 Dependence of Strouhal number St on gap spacing g^* .

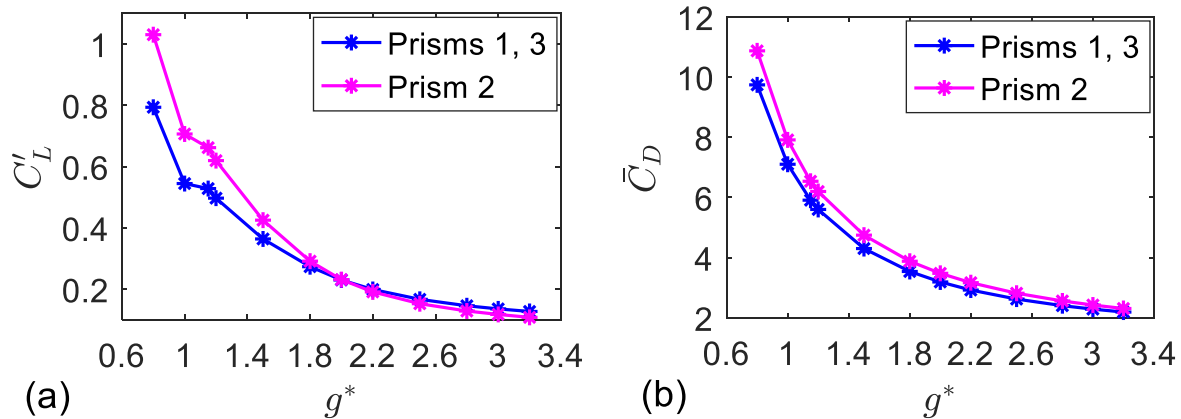


Fig. 3 Dependence on g^* of (a) fluctuating lift coefficient C'_L , and (b) time-mean drag coefficient \bar{C}_D .

The effects of g^* on C'_L and \bar{C}_D are depicted in Fig. 3. The variation in C'_L or \bar{C}_D exhibits the same nature as that in St (Fig. 2). The C'_L is smaller for prisms 1 and 3 than for prism 2 for $g^* < 2.15$. A reverse change occurs for $g^* \geq 2.15$. This happens as boundary layer on the wall remains attached for a larger distance, failing to interact with the vortices from outer prisms. For the same reason, the C'_L of the outer prisms becomes higher compared to that of the middle one. On the other hand, Fig 3(b) shows that the middle prism has higher \bar{C}_D than the outer prisms. Furthermore, the values of \bar{C}_D for three prisms approach each other with increase g^* because the wall effect on the prisms becomes negligible with g^* increasing.

4. CONCLUSIONS

The flow around three identical rectangular prisms in side-by-side arrangement in the presence of wall proximity is studied at a fixed Reynolds number 100. Special focus is given to the effect of gap spacing ratio g^* ($0.8 \leq g^* \leq 3.2$) on St , \bar{C}_D and C'_L . It is observed that at a fixed gap spacing the vortex shedding frequency is identical for three prisms. The St , \bar{C}_D and C'_L all decrease with g^* increasing. At a large g^* , the C'_L and \bar{C}_D of all three prisms approach each other as the influence of side walls on the prisms as well as the influence a prism on the others reduce.

ACKNOWLEDGMENTS

ALAM wishes to acknowledge the support given by the National Natural Science Foundation of China through Grants 11672096 and 91752112.

REFERENCES

Alam, M. M. and Zhou, Y. (2013) Intrinsic features of flow around two side-by-side square cylinders. *Phys. Fluids*. **25**, 085106.

- Alam, M. M., Zhou, Y. and Wang, X. W. (2011), "The wake of two side-by-side square cylinders," *J. Fluid Mech.* **669**,432-471.
- Agrawal, A., Djenidi, L. and Antonia, R.A. (2006), "Investigation of flow around a pair of side-by-side square cylinders using the lattice Boltzmann method," *Computers and Fluids*, **35**, 1093-1107.
- Camarri, S. and Giannetti, F. (2007), "On the inversion of the von Karman street in the wake of a confined square cylinder," *J. Fluid Mech*, **574**, 169-178.
- Davis, R.W., Moore, E.F. and Purteel, L.P. (1984), "A numerical-experimental study of confined flow around rectangular cylinders," *Phys Fluid*, **27**, 46-59.
- Kumar, S.R., Sharma, A. and Agrawal, A. (2008), "Simulation of flow around a row of square cylinders," *J Fluid Mech.*, **606**, 369-397.
- Sahu, A.K., Chhabra, R.P. and Eswaran, V. (2009), "Two-dimensional unsteady laminar flow of a power law fluid across a square cylinder," *J Non-Newtonian Fluid Mech*, **160**, 157-167.
- Sen, S., Mittal, S. and Biswas G. (2011), "Flow past a square cylinder at Low Reynolds numbers," *Int J Numer Meth Fluids*, **67**, 1160-1174.
- Sewatkar, C.M., Sharma, A. and Agrawal, A. (2009), "On the effect of Reynolds number for flow around a row of squire cylinders," *Phys. Fluids*, **21**, 083602.
- Sharma, A. and Eswaran, V. (2004), "Heat and Fluid Flow across a square cylinder in the two-dimensional laminar flow regime," *Num Heat Trans A*, **45**, 247-269.
- Singh, A.P., De, A.K., Carpenter, V.K., Eswaran, V. and Muralidhar, K. (2009), "Flow past a transversely oscillating square cylinder in free stream at low Reynolds numbers," *Int J Numer Meth Fluids*, **61**, 658-682.
- Sohankar, A.,Norberg C. and Davidson, L. (1998), "Low-Reynolds number flow around a square cylinder at incidence: study of blockage, onset of vortex shedding and outlet boundary condition," *Int J Numer Meth Fluids*, **26**, 39-56.
- Zheng, Q. and Alam, M.M. (2017), "Intrinsic features of flow past three square prisms in side-by-side arrangement," *J Fluid Mech.*, **826**, 996-1033.